Supporting Information

"Three-in-One" Nanocomposite as Multifunctional Nanozyme for Ultrasensitive Ratiometric Fluorescence Detection of Alkaline Phosphatase

Xuemei Li,[a] Mengchao Cai,[a], Zhiwei Shen,[a] Min Zhang,*[a], Zisheng Tang,[c,e,d,f,g] Shi-Hua Luo,*[h] and Na Lu*[a]

[a] School of Materials Engineering, Shanghai University of Engineering Science, Shanghai 201620, China

[b] College of Chemistry and Chemical Engineering, Shanghai University of Engineering Science, Shanghai 201620, China

[c] Department of Endodontics, Shanghai Ninth People's Hospital, Shanghai Jiao Tong University School of Medicine, Shanghai 200011, China

[d] College of Stomatology, Shanghai Jiao Tong University, Shanghai 200011, China

[e] National Center for Stomatology, Shanghai 200011, China

[f] National Clinical Research Center for Oral Diseases, Shanghai 200011, China

[g] Shanghai Key Laboratory of Stomatology, Shanghai 200011, China

[h] Department of Traumatology, Rui Jin Hospital, School of Medicine, Shanghai Jiao Tong University, Shanghai, 200025, China

E-mail addresses: zhangmin@sues.edu.cn (M. Zhang), jqab@163.com (S.-H. Luo), nlu2014@163.com (N. Lu).

Table of Contents

EXPERIMENTAL SECTION

Materials and chemicals. Alkaline phosphatase (ALP) was obtained from Sangon Biotech Co., Ltd. (Shanghai, China). Amplex Red (AR), curcumin (CUR), o-Phenylenediamine (OPD), L-Ascorbic acid 2-phosphate trisodium (AA2P), L-Ascorbic acid (AA), nitroblue tetrazoliun (NBT), methionine, riboflavin, and 30% H_2O_2 were purchased from Shanghai Titan Scientific Co., Ltd. (Shanghai, China). 2,2'-azino-bis(3-ethylbenzthiazoline)-6-sulfonic acid (ABTS), 3,3',5,5'-tetramethylbenzidine (TMB) was purchased from Sinopharm Chemical Reagent Co., Ltd. (Shanghai, China). Cerium (III) nitrate hexahydrate ($Ce(NO_3)_3 \cdot 6H_2O$), hexamethylenetetraminem (HMT), Potassium permanganate ($KMnO_4$), sodium acetate trihydrate ($NaAc \cdot 3H_2O$) , ferric chloride hexahydrate ($FeCl_3 \cdot 6H_2O$), 3,5-Di-tert-butylcatechol (3,5-DTBC, 98%), and dopamine were purchased from Aladdin (Shanghai, China). All chemicals were used without further purification. Ultrapure water with a resistivity of 18 $M\Omega \cdot cm^{-1}$ was used in the assays.

Table S1. Comparison of kinetic parameters of different enzyme-like activities.

Catalyst	Enzyme-like Activity	Substrate	K_m (mM)	V_{max} (10^{-8} M s^{-1})	Reference
Fef NCs	OXD	TMB	0.22	19.6	This work
^{a} CeO_2 NPs	OXD	TMB	1.50	6.9	1
^{b} MnO_2 NSs	OXD	TMB	0.062	425	2
Fef NCs	POD	H_2O_2	0.01	9.34	This work
Fe_3O_4 NPs	POD	H_2O_2	154	9.78	3
^{c} Fe_3O_4@C YSNs	POD	H_2O_2	0.27	12.0	4
Fef NCs	CAT	H_2O_2	0.72	210	This work
^{d}Mnf	CAT	H_2O_2	0.511	12000	5
Pd nanocubes	CAT	H_2O_2	102.4	220	6

^{a} CeO_2 NPs: CeO_2 nanoparticles; ^{b} MnO_2 NSs: MnO_2 nanosheets; ^{c} Fe_3O_4@C YSNs: Fe_3O_4@C yolk-shell nanostructures; ^{d} Mnf: Mn_3O_4 nanoparticles with flower-like morphology.

Table S2. Comparison of kinetic parameters of catechol oxidase-like activities.

Catalyst	Substrate	K_m (mM)	V_{max} (10^{-8} M s^{-1})	Reference
Fef NCs	3,5-DTBC	0.11	85	This work
	Dopamine	0.61	86	This work
MOF-818	3,5-DTBC	0.81	317	7
	Dopamine	0.48	8	7
CeO_2	3,5-DTBC	1.262	18.2	7
Pt NPs	3,5-DTBC	1.811	471	7
Catechol oxidase	3,5-DTBC	0.5	-	8

Table S3. Comparison of different methods for ALP detection.

Sensing system	Method	Linear range (mU/mL)	LOD (mU/mL)	Reference
PDA liposomes	Colorimetry	10-200	2.8	9
[a] N/S-CDs	Fluorescence	2.5-70	0.396	10
[b] Au/LDO	Colorimetry	4-60	1.35	11
Nucleotide coordinated copper ion	Colorimetry	10-30	0.3	12
	Fluorescence	1-30	0.45	
[c] RhB@Alg/Fe^{3+}	Visual detection	1-400	0.37	13
[d] AIEgen-peptide conjugate	Fluorescence	1-1000	1.2	14
[e] CDs /OPD	Fluorescence	5-350	3.6	15
[f] AgNPrs-Cu^{2+}	Distance measurement	5-50, 50-200	5	16
MnO_2 nanosheets	Fluorescence	0.25-10	0.06	17
dephosphorylation-initiated transcription reaction	Fluorescence	0.05-1	0.02	18
Phenyl phosphate	Electrochemistry	20-1500	3	19
Aminoferrocene labeled ssDNA	Electrochemistry	20-100	1.48	20
Fef NCs	Fluorescence	0.2-0.1	0.19	This work

[a] N/S-CDs: sulfur co-doped carbon dots; [b] Au/LDO: Au-decorated CoAl-layered double oxide nanozymes; [c] RhB@Alg/Fe^{3+}: alginate hydrogel crosslinked with Fe^{3+} and rhodamine B (RhB); [d]AIEgens: aggregation-induced emission luminogens; [e] CDs /OPD: carbon dots o-phenylenedi-amine; [f] AgNPrs-Cu^{2+}: silver hexagonal nanoprism-Cu^{2+}.

Table S4. Recovery Analysis of ALP in Human Serum Samples.

No.	Added (mU/mL)	Total detected (mU/mL)	Recovery (%)	RSD (%)
Samples 1	0	0.11		
	0.5	0.63	102%	2.3%
	1	1.10	99%	0.4%
Samples 2	0	0.30		
	0.5	0.77	94.6%	3.3%
	1	1.31	101%	0.7

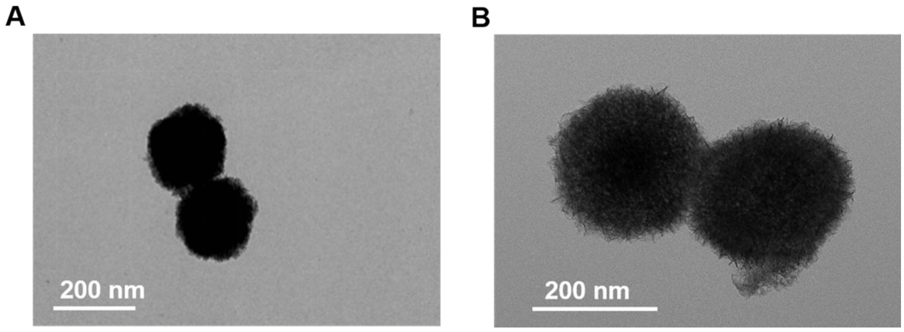

Figure S1. TEM images of (A) Fe_3O_4 nanoparticles (NPs) and (B) Fe_3O_4@MnO_2 nanocomposites (NCs).

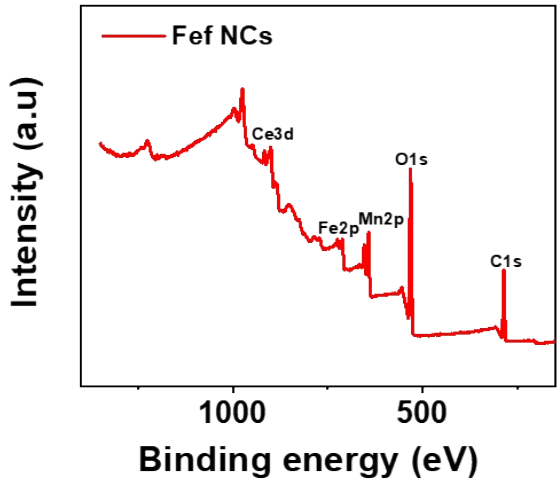

Figure S2. XPS spectrum of Fef NCs.

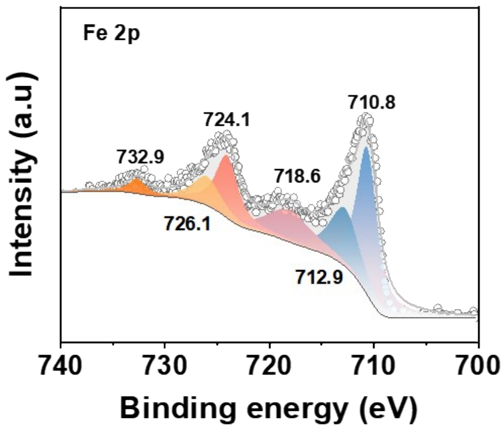

Figure S3. XPS spectra of Fe 2p for Fef NCs.

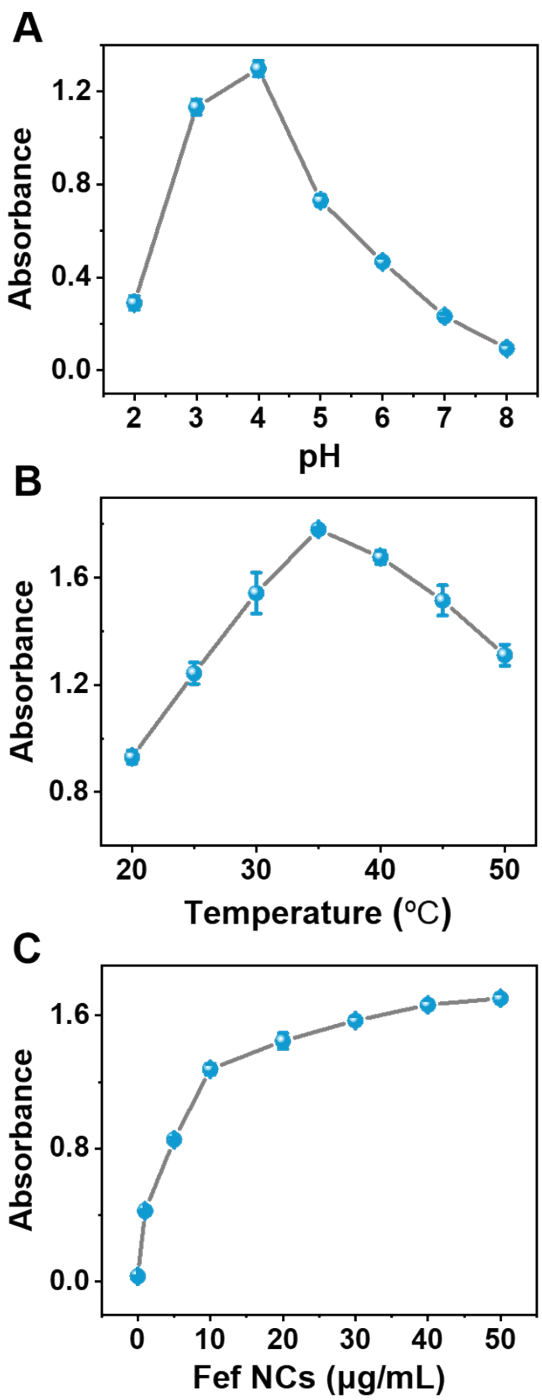

Figure S4. Dependence of OXD-like activities on (A) pH, (B) temperature, and (C) the concentrations of Fef NCs.

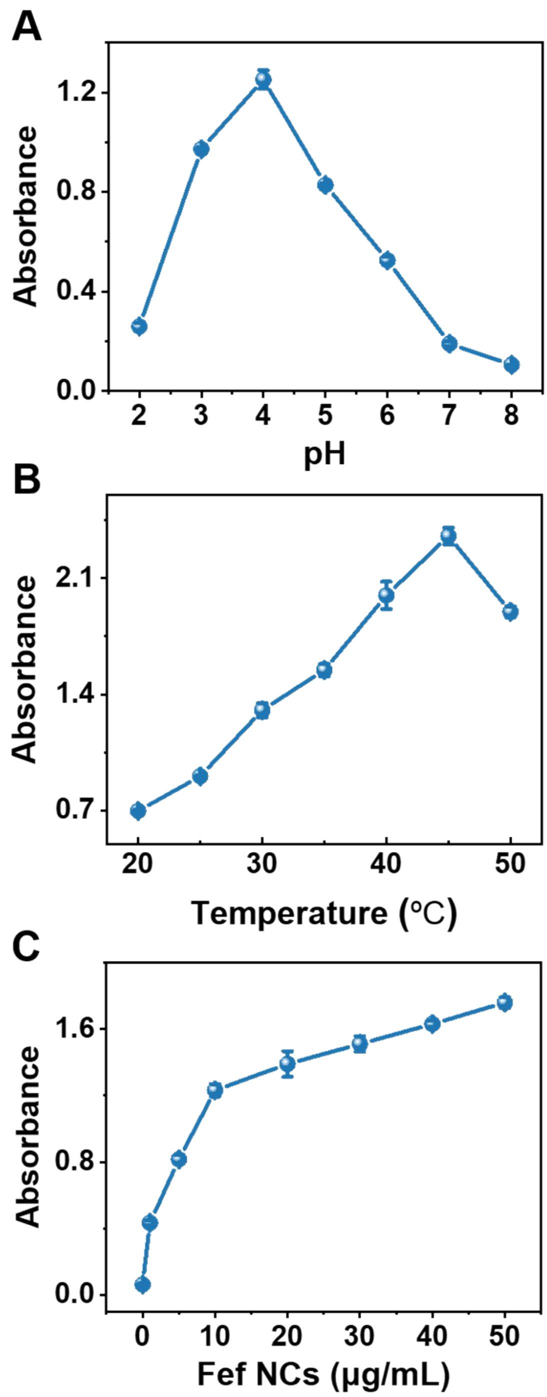

Figure S5. Dependence of POD-like activities on (A) pH, (B) temperature, and (C) the concentrations of Fef NCs.

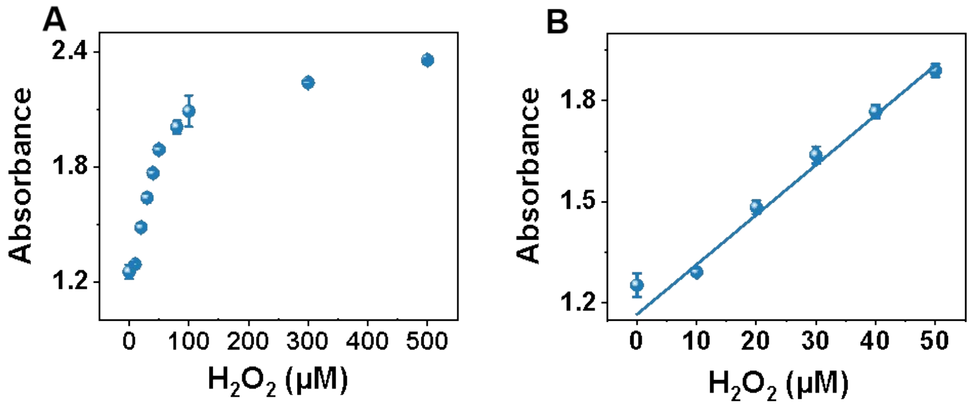

Figure S6. H_2O_2 detection based on POD-like activity of Fef NCs. (A) Relationship between the absorbance and the concentrations of H_2O_2. (B) Linear calibration curve for H_2O_2 detection.

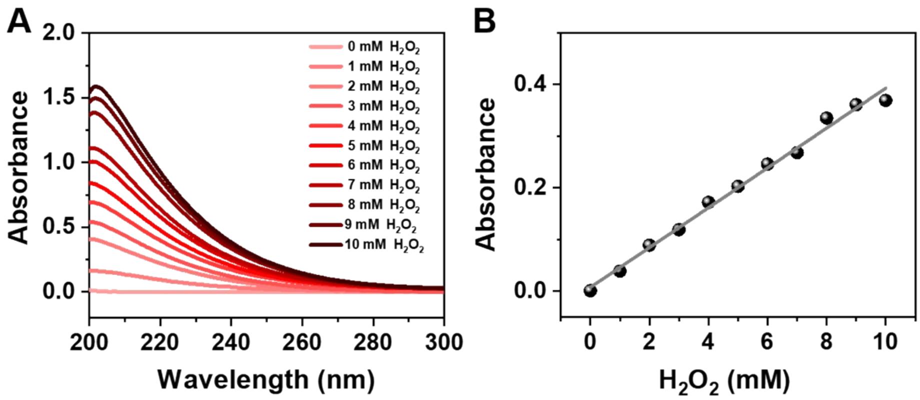

Figure S7. H_2O_2 decomposition based on CAT-like activity of Fef NCs. (A) UV-Vis absorption spectra with increasing H_2O_2 concentrations. (B) Linear relationship between the absorbance at 240 nm and the concentration of H_2O_2.

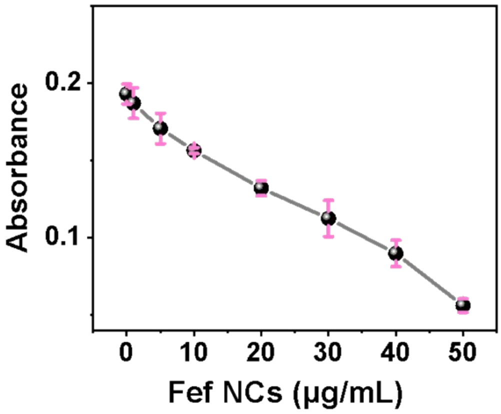

Figure S8. Dependence of the CAT-like activity on the concentration of Fef NCs

	a	b	c	d	e	f	g	h	i
Riboflavin	−	−	−	−	+	+	+	+	+
Methionine	−	+	−	−	−	+	+	+	+
NBT	−	−	+	−	−	+	+	+	+
Fef NCs	−	−	−	+	−	+	+	−	−
PB	+	+	+	+	+	+	+	+	+
Light	+	+	+	+	+	−	+	−	+

Figure S9. SOD-like activity of Fef NCs. Photograph of different reaction systems.

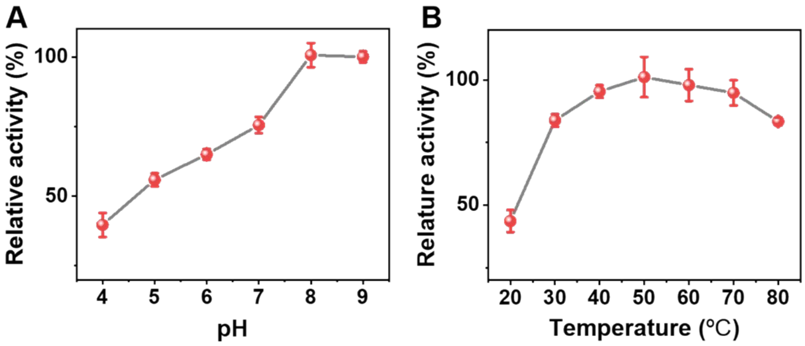

Figure S10. Dependence of catechol oxidase-like activities of Fef NCs on (A) pH and (B) temperature.

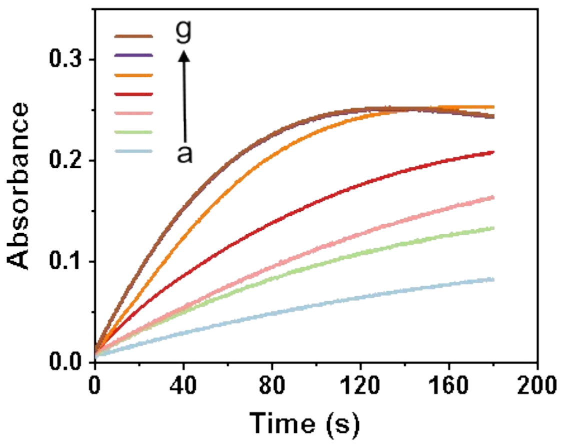

Figure S11. Time-dependent absorbance of aminochrome upon the addition of varying concentrations of Fef NCs (From a to g: 1, 5, 10, 20, 30, 40, and 50 μg/mL).

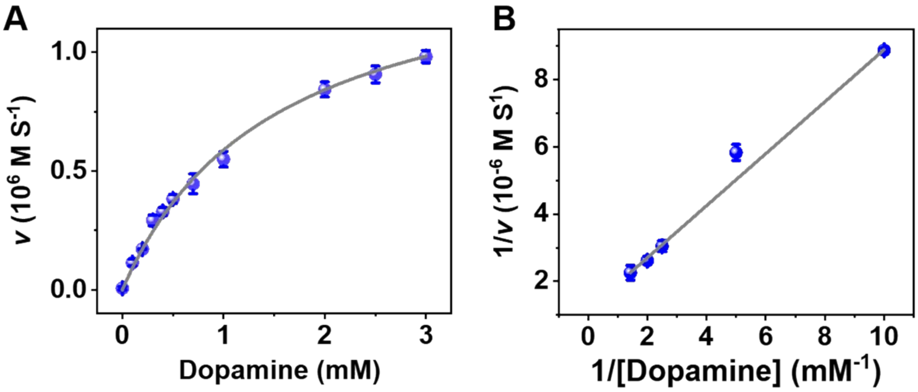

Figure S12. Steady-state kinetic assays of catechol oxidase-like activities by varying concentrations of dopamine. (A) Michaelis-Menten curve of Fef NCs for Dopamine. (B) The Lineweaver-Burk plot of the double reciprocal of the Michaelis-Menten equation.

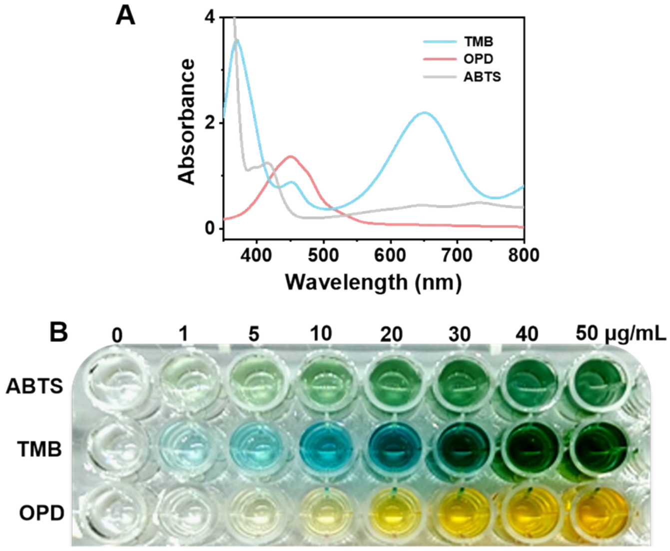

Figure S13. The OXD-like activity of Fef CNs was applied to different kinds of colorimetric substrates, including TMB, ABTS, and OPD. (A) UV-Vis absorption spectra of different oxidized substrates in dissolved oxygen in the presence of Fef CNs at room temperature. (B) Photograph of different substrate reaction solutions with varying concentrations of Fef NCs.

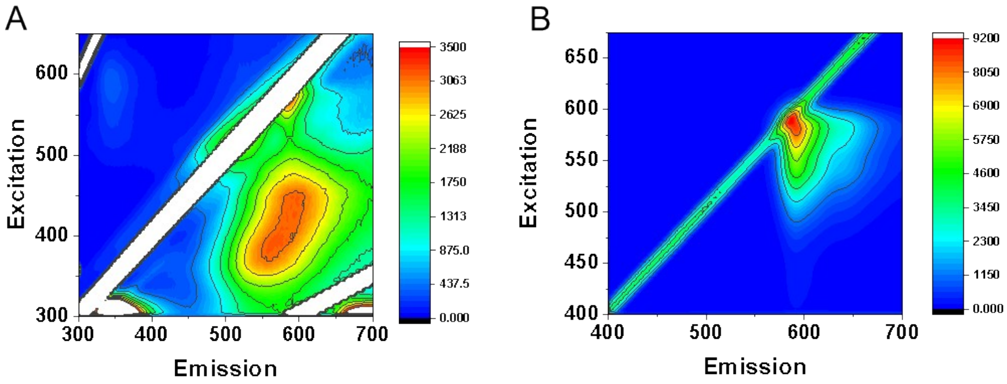

Figure S14. Three-dimensional fluorescence spectra of (A) ARox and (B) CUR.

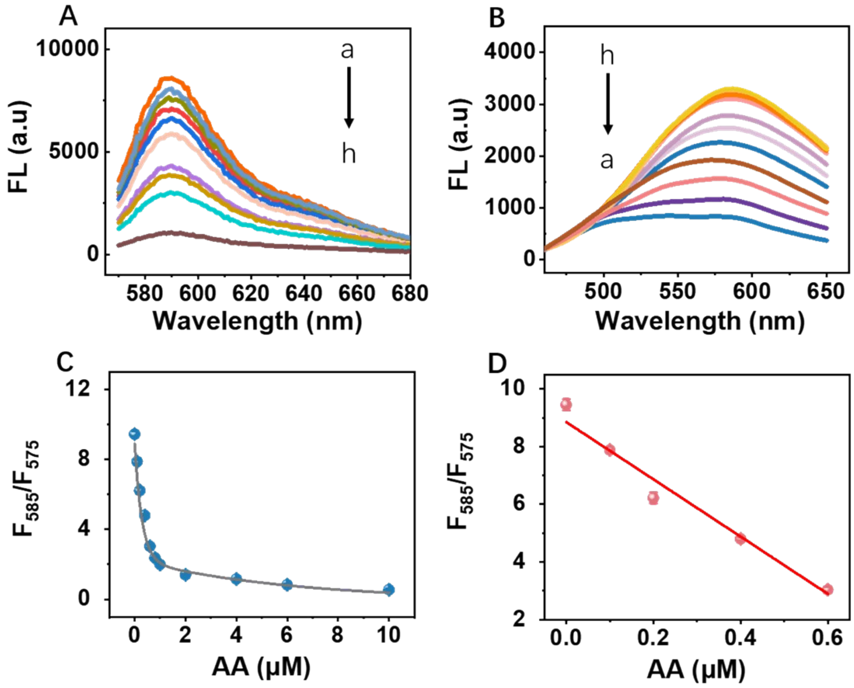

Figure S15. Ratiometric fluorescence detection of AA by using Fef NCs. (A, B) Fluorescence spectra of AR (A) and CUR (B) with different concentrations of AA (From a to h: 0, 0.1, 0.2, 0.4, 0.6, 0.8,1,2,4,6, and 10 μM). (C) Relationship between the fluorescence ratio (F_{585}/F_{575}) and the concentrations of AA. (D) Linear calibration curve for AA detection.

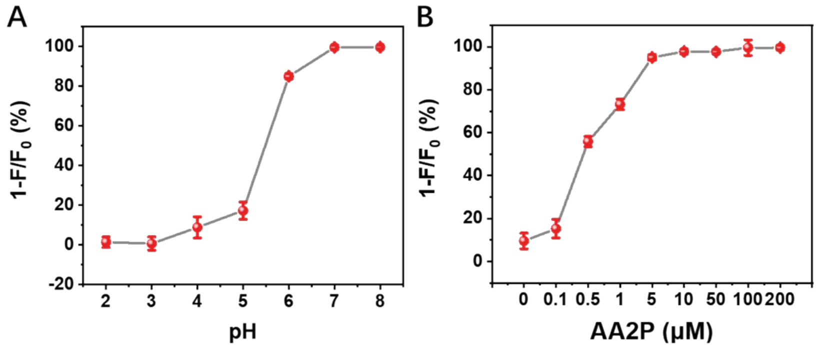

Figure S16. Optimization of experimental conditions for ALP detection. (A) Fluorescence response of AR catalyzed by Fef NCs under different pH. (B) Fluorescence response of AR catalyzed by Fef NCs with varying concentration of AA2P. [Fef NCs] = 100 μg/mL, [ALP] = 40 mU/mL.

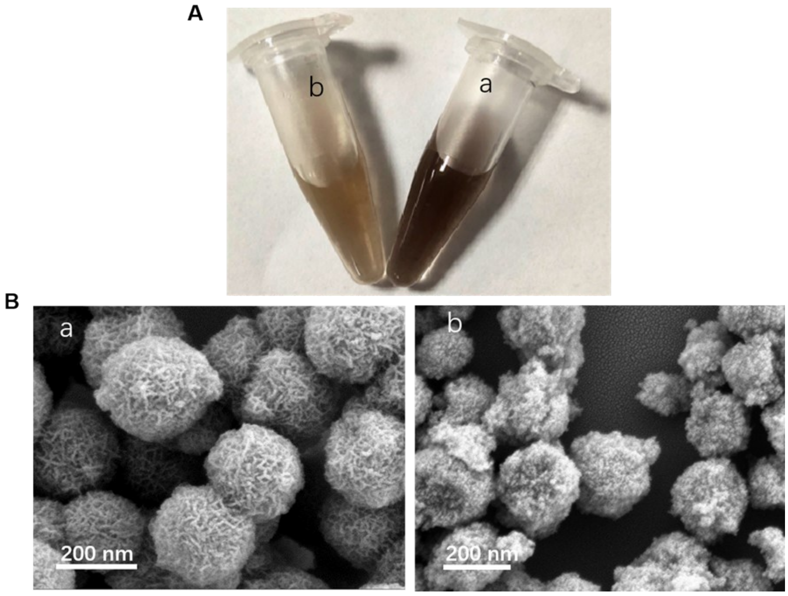

Figure S17. (A) Photograph of the reaction solutions and (B) SEM images of Fef NCs before (a) and after (b) the ratiometric fluorescence detection of ALP.

References

1 B. Liu, Z. Huang and J. Liu, *Nanoscale*, 2016, **8**, 13562-13567.

2 J. Liu, L. Meng, Z. Fei, P. J. Dyson and L. Zhang, *Biosens. Bioelectron.*, 2018, **121**, 159-165.

3 L. Gao, J. Zhuang, L. Nie, J. Zhang, Y. Zhang, N. Gu, T. Wang, J. Feng, D. Yang, S. Perrett and X. Yan, *Nat. Nanotechnol.*, 2007, **2**, 577-583.

4 N. Lu, M. Zhang, L. Ding, J. Zheng, C. Zeng, Y. Wen, G. Liu, A. Aldalbahi, J. Shi, S. Song, X. Zuo and L. Wang, *Nanoscale*, 2017, **9**, 4508-4515.

5 N. Singh, M. A. Savanur, S. Srivastava, P. D'Silva and G. Mugesh, *Angew. Chem. Int. Ed. Engl.*, 2017, **56**, 14267-14271.

6 C. Ge, G. Fang, X. Shen, Y. Chong, W. G. Wamer, X. Gao, Z. Chai, C. Chen and J. J. Yin, *ACS Nano*, 2016, **10**, 10436-10445.

7 M. Li, J. Chen, W. Wu, Y. Fang and S. Dong, *J. Am. Chem. Soc.*, 2020, **142**, 15569-15574.

8 A. Rompel, H. Fischer, D. Meiwes, K. Büldt-Karentzopoulos, A. Magrini, C. Eicken, C. Gerdemann and B. Krebs, *FEBS Lett.*, 1999, **445**, 103-110.

9 D.-E. Wang, S. You, W. Huo, X. Han and H. Xu, *Microchimica Acta*, 2022, **189**, 70.

10 Y. Zhan, S. Yang, L. Chen, Y. Zeng, L. Li, L. Zhenyu, L. Guo and W. Xu, *ACS Sustainable Chemistry & Engineering*, 2021, **9**.12922–12929.

11 X. Liu, X. Mei, J. Yang and Y. Li, *ACS Appl. Mater. Interfaces*, 2022, **14**, 6985-6993.

12 H. Huang, J. Bai, J. Li, L. Lei, W. Zhang, S. Yan and Y. Li, *J Mater Chem B*, 2019, **7**, 6508-6514.

13 L. Gao, Y. Li, Z.-Z. Huang and H. Tan, *Anal. Chim. Acta*, 2021, **1148**, 238193.

14 L. Zhang, Y. Li, G. Mu, L. Yang, C. Ren, Z. Wang, Q. Guo, J. Liu and C. Yang, *Anal. Chem.*, 2022, **94**, 2236-2243.

15 Y. Zhu, X. Tong, Q. Wei, G. Cai, Y. Cao, C. Tong, S. Shi and F. Wang, *Biosens. Bioelectron.*, 2022, **196**, 113691.

16 K. Phoonsawat, K. Khachornsakkul, N. Ratnarathorn, C. S. Henry and W. Dungchai, *ACS Sens*, 2021, **6**, 3047-3055.

17 R. Wang, Z. Wang, H. Rao, X. Xue, M. Luo, Z. Xue and X. Lu, *Chem. Commun. (Camb.)*, 2021, **57**, 4444-4447.

18 F. Ma, W.-j. Liu, L. Liang, B. Tang and C.-Y. Zhang, *Chem. Commun. (Camb.)*, 2018, **54**, 2413-2416.

19 L. Sappia, B. Felice, M. A. Sanchez, M. Martí, R. Madrid and M. I. Pividori, *Sens. Actuators B Chem.*, 2019, **281**, 221-228.

20 W. Wang, J. Lu, L. Hao, H. Yang, X. Song and F. Si, *Anal. Bioanal. Chem.*, 2021, **413**, 1827-1836.